Structural Transitions in Sodium Chloride Nanocrystals

Robert R. Hudgins, Philippe Dugourd,* Jason M. Tenenbaum, and Martin F. Jarrold
Department of Chemistry, Northwestern University, 2145 Sheridan Road, Evanston, Illinois 60208
(Received 30 January 1997)

High resolution ion mobility measurements have been used to examine structural transitions in $(NaCl)_nCl^-$ nanocrystals with between 30 and 40 NaCl units. Transformations between bulk fragment geometries with different $j \times k \times l$ dimensions are observed at ambient temperatures. In some of these transformations, close to half the atoms are relocated, yet the Arrhenius activation energies are less than 0.6 eV. A surface diffusion mechanism is proposed to explain the remarkably low activation energies. [S0031-9007(97)03225-0]

PACS numbers: 61.46.+w, 36.40.Sx

Structural rearrangements in atomic and molecular clusters have been studied both theoretically [1–4] and experimentally [5–8], particularly in relation to phase transitions in bulk materials. However, despite numerous studies there is little quantitative information available. Here, we describe direct measurements of the Arrhenius activation energies for structural transitions in NaCl nanocrystals. $(NaCl)_nCl^-$ clusters with more than 30 NaCl units undergo transitions between bulk fragment geometries with different $j \times k \times l$ dimensions. Some of these transitions involve the relocation of close to half the atoms in the cluster, yet they occur at ambient temperatures. Arrhenius activation energies have been determined for the structural transitions by measuring the isomerization rates as a function of temperature. The low activation energies for these processes are attributed to a surface diffusion mechanism, which may be an important mechanism for low temperature structural transitions in a wide range of clusters and nanocrystals.

Alkali halide clusters are interesting model systems because the bulk structural motif emerges at small cluster sizes [9–11]. They can be modeled with a relatively simple potential [10], and there have been many theoretical investigations of alkali halide structural transitions [2,12–18]. For example, Fatemi *et al.* [19] have recently employed photoelectron spectroscopy to probe the isomerization between a hexagonal ring structure and an incomplete $2 \times 2 \times 2$ cube for $(CsX)_3Cs^-$ clusters. Evidence for the isomerization of larger sodium chloride clusters has been inferred from photodetachment and mass spectrometry experiments [20,21]. In our studies, the isomerization processes are probed by ion mobility measurements where the different isomers are separated on the basis of their different mobilities [22]. Our experiments are performed in 500 Torr helium buffer gas and have a time scale of hundreds of milliseconds, so the temperature is well defined.

The high resolution ion mobility apparatus employed for these studies has recently been described in detail [23]. The apparatus consists of a source region attached directly to a 63 cm long drift tube, followed by a mass spectrometer, and an ion detector. $(NaCl)_nCl^-$ clusters were produced by laser vaporization of a sodium chloride rod in a helium buffer gas. The source region and the drift tube are connected by a cylindrical ion gate, 2.5 cm long and 0.5 cm in diameter. A flow of helium buffer gas prevents neutral clusters from entering the drift tube, while an electric field pulls the ions through the ion gate against the flow. The voltage across the drift tube is 2–14 kV; the drift tube and source region contain helium buffer gas at a pressure of around 500 Torr. At the end of the drift tube, some of the ions exit through a 0.125 mm hole. They are focused into a quadrupole mass spectrometer, mass analyzed, and then detected. Drift time distributions are recorded with a multichannel scaler using the source laser pulse as the start trigger.

Figure 1 shows drift time distributions measured for $(NaCl)_{36}Cl^-$ at room temperature. The three peaks in the distributions correspond to different structural isomers that have been separated by their different mobilities. Structural assignments for the isomers observed for these clusters have been reported in a recent publication [24]. In brief, structures are optimized using an ionic potential with polarization effects [25,26] with parameters taken from Welch *et al.* [27]. Mobilities are then calculated for these structures and compared with the experimental values. In Fig. 1, the peak on the left has been assigned to a $5 \times 4 \times 4$ fcc cuboid with an incomplete face, the middle peak has been assigned to an incomplete $5 \times 5 \times 3$ cuboid, and the peak on the right to an incomplete $6 \times 5 \times 3$ cuboid. By varying the drift voltage, one can vary the time that the ions spend in the drift tube. Drift voltages of (a) 10.5 kV, (b) 4.0 kV, and (c) 1.95 kV were employed for the distributions shown in Fig. 1. The average drift times increase from 120 to 640 ms as the drift voltage is lowered. The abundance of the incomplete $6 \times 5 \times 3$ geometry, the peak on the right in the figure, decreases as the residence time is increased, indicating that this structure is converting into another structure as it travels through the drift tube. The intensity between the peak on the right and the peaks on the left results from $(NaCl)_{36}Cl^-$ isomers that interconvert at different positions along the length of the drift tube. If an isomer *B* converts into

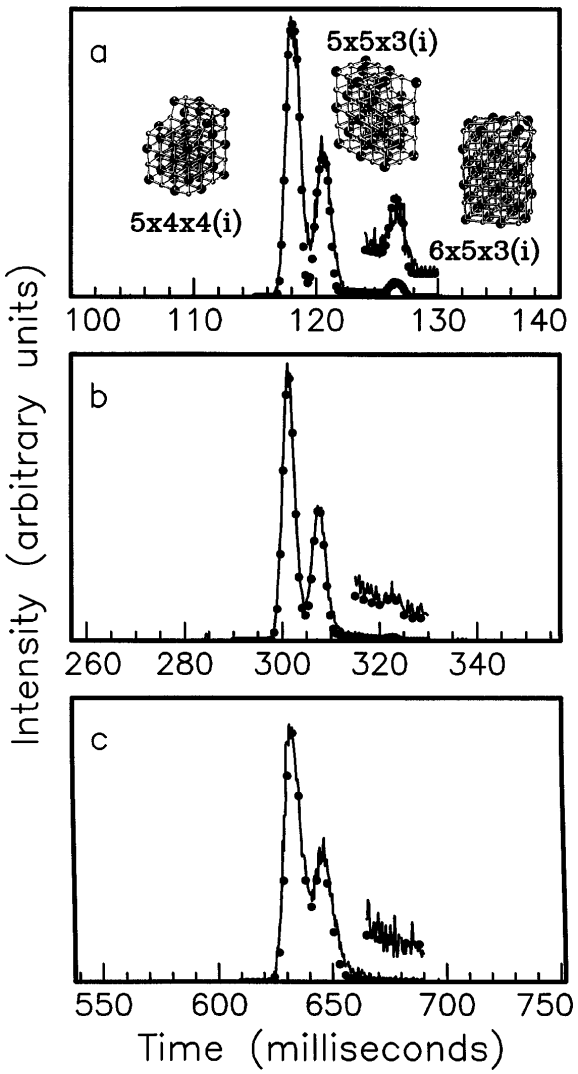

FIG. 1. Drift time distributions recorded for $(NaCl)_{36}Cl^-$ at room temperature with drift voltages of (a) 10.5 kV, (b) 4 kV, and (c) 1.95 kV. The geometries shown in the figure are described in the text. The peak assigned to the $6 \times 5 \times 3$ geometry is shown multiplied by a factor of 5. The simulations used to extract the rate constant are superimposed on each distribution as black dots.

isomer A as it travels through the drift tube, it will occur between the peaks due to A and B because it spends part of its time as A and part as B. Note that the depletion of the peak assigned to the $6 \times 5 \times 3$ geometry cannot be due to electron detachment [28] or dissociation [29]. The activation energies for these processes are greater than 2 eV, and so the probability of them occurring at ambient temperatures is vanishingly small.

Rate constants for the thermally activated structural transformations can be obtained from the results shown in Fig. 1 by simulating the drift time distributions. For two isomers A and B, the drift time distribution is given by

$$\Phi(t) = \int \rho(t) g(t, t')\, dt'$$

with $\rho(t)$ and $g(t, t')$ given by

$$\rho(t) = A_0 \delta(t - L/\nu_A) + B_0 \delta(t - L/\nu_B) e^{-kt} + \int_0^t B_0 \delta\left(t - \tau - \frac{L - \nu_B \tau}{\nu_A}\right) e^{-k\tau} k\, d\tau ,$$

$$g(t, t') = \frac{\nu_A}{\sqrt{Dt}}\, e^{-(t-t')^2 \nu_A^2 / 4Dt} .$$

The function $\rho(t)$ has three terms that describe the peak for isomer A, the peak for isomer B, and the region between the two peaks due to B converting into A along the length of the drift tube. The function $g(t, t')$ accounts for the diffusional broadening of the ion packet [30]. Broadening due to the initial spatial distribution of the ion packet is also accounted for, though this is not shown in the equations. The drift time distribution is thus described in terms of the drift tube length L, the drift velocities v_A and v_B of isomers A and B, the initial intensities A_0 and B_0, D, the diffusion constant for the ions, and k, the isomerization rate constant. D, v_A, and v_B are extracted directly from the drift time distributions. Thus only A_0, B_0, and k are variables in the equations, for a given distribution. By fixing the ratio A_0/B_0, one can describe the distribution in terms of only k.

The black dots overlaid on the distributions for $(NaCl)_{36}Cl^-$ in Fig. 1 show the fit to the data with $k = 7.1\ s^{-1}$. A value of $7.1\ s^{-1}$ corresponds to a half-life of 100 ms, and from Figs. 1(a) and 1(b), one can see that the peak on the right is reduced by around a factor of 4 over the course of ~2 half-lives. A similar analysis has been performed for $(NaCl)_{30}Cl^-$, $(NaCl)_{35}Cl^-$, $(NaCl)_{36}Cl^-$, and $(NaCl)_{37}Cl^-$ at various temperatures between 7 °C and 77 °C. Figure 2 shows the fits to the drift time distributions for $(NaCl)_{35}Cl^-$ at three temperatures, with a fixed drift voltage of 7 kV. For $(NaCl)_{35}Cl^-$ there are three isomers present, which have been assigned to an incomplete $5 \times 5 \times 3$, an incomplete $5 \times 4 \times 4$, and an $8 \times 3 \times 3$ geometry with a single defect, on the basis of the calculated mobilities for these geometries. The $8 \times 3 \times 3$ and $5 \times 5 \times 3$ geometries convert into the $5 \times 4 \times 4$ geometry. The simulations for this cluster were performed using the format described above, but with additional terms in $\rho(t)$ for the additional isomer. It is clear from the results shown in Fig. 2 that the isomerization rate increases as the temperature is raised. For the $8 \times 3 \times 3$ to $5 \times 4 \times 4$ transition the rate constants obtained from the simulations are 0.9 ± 0.3, 8.0 ± 0.5, and $60 \pm 3\ s^{-1}$ at 7 °C, 33 °C, and 67 °C, and for the $5 \times 5 \times 3$ to $5 \times 4 \times 4$ transition the rate constants are 1.4 ± 0.2, 8.0 ± 1.0, and $25 \pm 3\ s^{-1}$.

For a thermally activated process, the rate constants should follow the Arrhenius equation $k = A \exp(-E_A/k_B T)$, where A is the frequency factor, k_B is the Boltzmann constant, T is the temperature, and E_A is the activation energy. The activation energy can be obtained from a plot of $\ln k$ vs $(k_B T)^{-1}$. Such a plot is shown in Fig. 3 for transformation of the $(NaCl)_{35}Cl^-$ $8 \times 3 \times 3$ geometry into the $5 \times 4 \times 4$ geometry. An activation

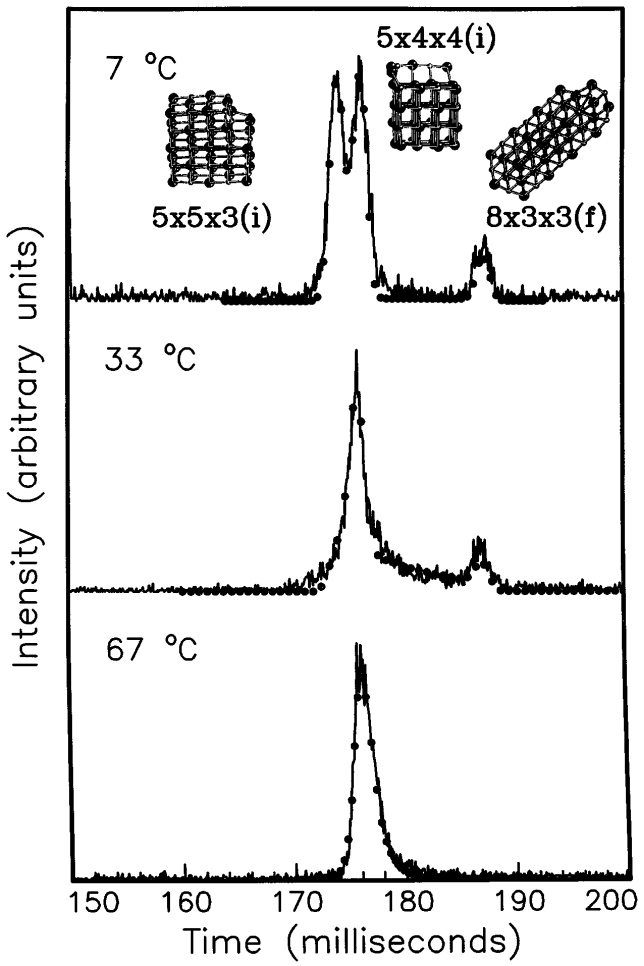

FIG. 2. Drift time distributions for $(NaCl)_{35}Cl^-$ at 7 °C, 33 °C, and 67 °C, with a drift voltage of 7 kV. The geometries shown in the figure are described in the text. The simulations used to extract the rate constants are superimposed on each distribution as black dots.

energy of 0.57 ± 0.05 eV is obtained. Activation energies for the other transitions we have studied are given in Table I. The activation energies are between 0.3 and 0.6 eV. The values determined for the frequency factor A are all on the order of 10^6 to 10^{10} s^{-1}. The frequency factor for a simple molecular process is expected to be on the order of a vibrational frequency 10^{12} to 10^{14} s^{-1} [31].

The isomerization of NaCl and other alkali halide clusters has been examined theoretically by several groups [2,12–18]. Activation energies have been reported only for clusters with less than 10 atoms. For NaCl clusters the values range from 0.25 to 0.60 eV [12,13,18]. These are similar to the values we have obtained for the 60–80 atom clusters studied here. However, it is probably not appropriate to compare them to our results because the structural transformations for the larger clusters studied here are much more complicated than the isomerization processes of the small clusters, where only a limited number of conformations exist.

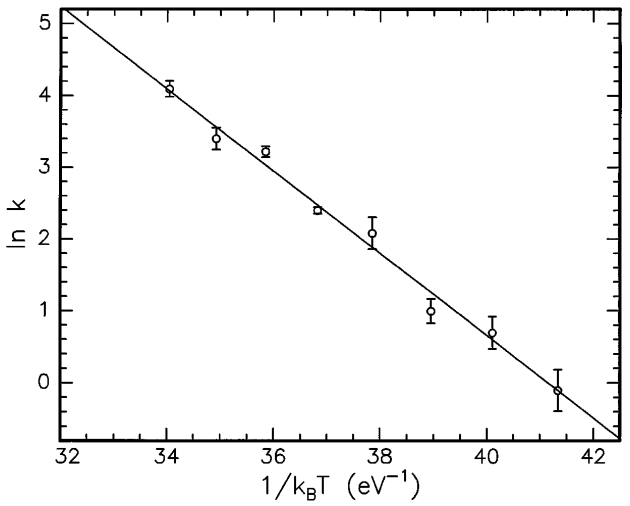

FIG. 3. Arrhenius plot for the conversion of the $(NaCl)_{35}Cl^-$ $8 \times 3 \times 3$(f) structure to a $5 \times 4 \times 4$(i) structure.

For bulk NaCl, the measured activation energies for the migration of an ion vacancy through the solid is 0.85 eV [32]. The activation energies in Table I are all less than 0.6 eV, so the mechanism by which the $(NaCl)_nCl^-$ clusters transform their shapes is less energetically hindered than this process. Diffusion along a surface is intuitively less hindered than through a volume, but experimental studies on surface diffusion have mostly been limited to metals [33]. However, theoretical studies predict activation energies of surface diffusion on bulk NaCl to be less than 0.5 eV along the least-hindered route [34]. Thus, a likely mechanism for the observed structural transformations is a sequence of surface diffusion steps.

The low values for the frequency factor A are consistent with a single highly concerted step, as well as mechanism involving a sequence of steps. It is unlikely under these conditions that such a large geometry change could be accomplished in a single concerted step, with such a small activation energy. However, a structural transformation effected through a series of surface diffusion steps could result in a frequency factor comparable to the measured

TABLE I. Activation energies for transitions between some NaCl cluster geometries. The geometries are identified by their $j \times k \times l$ dimensions. The letters c, f, and i following the $j \times k \times l$ dimensions indicate a complete cuboid, and cuboid with one vacancy (or F center), and a cuboid with an incomplete face, respectively.

Cluster	Converting isomer geometry	Product isomer geometry	Activation energy (eV)
$(NaCl)_{30}Cl^-$	$7 \times 3 \times 3$ i	$4 \times 4 \times 4$ i	0.57 ± 0.05
$(NaCl)_{35}Cl^-$	$8 \times 3 \times 3$ f	$5 \times 4 \times 4$ i	0.57 ± 0.05
$(NaCl)_{35}Cl^-$	$5 \times 5 \times 3$ i	$5 \times 4 \times 4$ i	0.53 ± 0.05
$(NaCl)_{36}Cl^-$	$6 \times 5 \times 3$ i	$5 \times 4 \times 4$ i	0.44 ± 0.05
$(NaCl)_{37}Cl^-$	$6 \times 5 \times 3$ i	$5 \times 5 \times 3$ c	0.36 ± 0.05

ones. Although, studies of self-diffusion on tungsten show that the frequency factors can vary by nine orders of magnitude, depending on the details of the mechanism [35].

In summary, we have determined Arrhenius activation energies for structural transitions in a number of NaCl nanocrystals. Unlike the isomerization processes that have been studied for smaller clusters, the structural transitions studied here are between geometries with the same structural motif but different $j \times k \times l$ dimensions. These are the cluster analog of a spontaneous change in the shape of a crystal. The activation energies determined for the structural transitions are remarkably low, 0.3 to 0.6 eV. Such low activation energies are consistent with the transitions occurring through a sequence of surface diffusion steps. It is likely that surface diffusion is an important mechanism for low temperature structural transitions in a wide range of clusters and nanocrystals.

We gratefully acknowledge the National Science Foundation (CHE-9306900) for support of this work. Ph. Dugourd also acknowledges financial support from CNRS and NATO.

*Permanent address: Laboratoire de Spectrometrie Ionique et Moleculaire (UMR n°5579), CNRS et Universite Lyon I, 43 bd du 11 novembre 1918, 69622 Villeurbanne Cedex, France.

[1] R. S. Berry, T. L. Beck, H. L. Davis, and J. Jellinek, Adv. Chem. Phys. **70**, 75 (1988).
[2] J. Luo, U. Landman, and J. Jortner, in *Physics and Chemistry of Small Clusters*, edited by P. Jena, B. K. Rao, and S. N. Khanna (Plenum, New York, 1987), p. 201.
[3] D. J. Wales and R. S. Berry, Phys. Rev. Lett. **73**, 2875 (1994).
[4] J. P. Rose and R. S. Berry, J. Chem. Phys. **98**, 3246 (1993).
[5] T. P. Martin, U. Näher, H. Schaber, and U. Zimmermann, J. Chem. Phys. **100**, 2322 (1994).
[6] U. Buck and I. Ettischer, J. Chem. Phys. **100**, 6974 (1994).
[7] A. J. Stace, Chem. Phys. Lett. **99**, 470 (1983); R. Knochenmuss, D. Ray, and W. P. Hess, J. Chem. Phys. **100**, 44 (1994).
[8] J. M. Hunter, J. L. Fye, M. F. Jarrold, and J. E. Bower, Phys. Rev. Lett. **73**, 2063 (1994).
[9] J. E. Campana, T. M. Barlak, R. J. Colton, J. J. Decorpo, J. R. Wyatt, and B. I. Dunlap, Phys. Rev. Lett. **47**, 1046 (1981).
[10] See T. P. Martin, Phys. Rep. **95**, 167 (1983).
[11] For a review, see R. L. Whetten, Acc. Chem. Res. **26**, 49 (1993).
[12] T. P. Martin, J. Chem. Phys. **72**, 3506 (1980).
[13] A. Heidenreich, J. Jortner, and I. Oref, J. Chem. Phys. **97**, 197 (1992).
[14] U. Landman, D. Scharf, and J. Jortner, Phys. Rev. Lett. **54**, 1860 (1985).
[15] D. Scharf, J. Jortner, and U. Landman, J. Chem. Phys. **87**, 2716 (1987).
[16] J. P. Rose and R. S. Berry, J. Chem. Phys. **96**, 517 (1992).
[17] V. K. W. Cheng, J. P. Rose, and R. S. Berry, Z. Phys. D **26**, 195 (1993).
[18] K. K. Sunil and K. D. Jordan, Chem. Phys. Lett. **164**, 509 (1989).
[19] D. J. Fatemi, F. K. Fatemi, and L. A. Bloomfield, Phys. Rev. A **54**, 3674 (1996).
[20] P. Labastie, J.-M. L'Hermite, Ph. Poncharal, and M. Sence, J. Chem. Phys. **103**, 6362 (1995).
[21] E. C. Honea, M. L. Homer, and R. L. Whetten, Phys. Rev. B **47**, 7480 (1993).
[22] D. F. Hagen, Anal. Chem. **51**, 870 (1979); Z. Karpas, R. M. Stimac, and Z. Rappoport, Int. J. Mass Spectrom. Ion Proc. **83**, 163 (1988); G. von Helden, M. T. Hsu, P. R. Kemper, and M. T. Bowers, J. Chem. Phys. **95**, 3835 (1991).
[23] Ph. Dugourd, R. R. Hudgins, D. E. Clemmer, and M. F. Jarrold, Rev. Sci. Instrum. **68**, 1122 (1997).
[24] Ph. Dugourd, R. R. Hudgins, and M. F. Jarrold, Chem. Phys. Lett. **267**, 186 (1997).
[25] J. Diefenbach and T. P. Martin, J. Chem. Phys. **83**, 4585 (1985).
[26] N. G. Phillips, C. W. S. Conover, and L. A. Bloomfield, J. Chem. Phys. **94**, 4980 (1991).
[27] D. O. Welch, O. W. Lazareth, G. J. Dienes, and R. D. Hatcher, J. Chem. Phys. **64**, 835 (1976).
[28] E. C. Honea, M. L. Homer, P. Labastie, and R. L. Whetten, Phys. Rev. Lett. **63**, 394 (1989).
[29] D. O. Welch, O. W. Lazereth, G. J. Dienes, and R. D. Hatcher, J. Chem. Phys. **68**, 2159 (1978).
[30] E. A. Mason and E. W. McDaniel, *Transport Properties of Ions in Gases* (Wiley, New York, 1988).
[31] S. W. Benson, *The Foundation of Chemical Kinetics* (McGraw-Hill, New York, 1960).
[32] H. W. Etzel and R. J. Maurer, J. Chem. Phys. **18**, 1003 (1950).
[33] A. Kapoor, R. T. Wang, and C. Wong, Catal. Rev. Sci. Eng. **31**, 129 (1989).
[34] V. K. W. Cheng, B. A. W. Coller, and E. R. Smith, J. Chem. Soc. Faraday Trans. 1 **84**, 899 (1988).
[35] W. R. Graham and G. Ehrlich, Phys. Rev. Lett. **31**, 1407 (1973).